

This is a self-archived version of an original article. This version may differ from the original in pagination and typographic details.

Author(s): Mattola, Salla; Hakanen, Satu; Salminen, Sami; Aho, Vesa; Mäntylä, Elina; Ihalainen, Teemu O.; Kann, Michael; Vihinen-Ranta, Maija

Title: Concepts to Reveal Parvovirus–Nucleus Interactions

Year: 2021

Version: Published version

Copyright: © 2021 the Authors

Rights: CC BY 4.0




Rights url: <https://creativecommons.org/licenses/by/4.0/>

Please cite the original version:

Mattola, S., Hakanen, S., Salminen, S., Aho, V., Mäntylä, E., Ihalainen, T. O., Kann, M., & Vihinen-Ranta, M. (2021). Concepts to Reveal Parvovirus–Nucleus Interactions. *Viruses*, 13(7), Article 1306. <https://doi.org/10.3390/v13071306>

Review

Concepts to Reveal Parvovirus–Nucleus Interactions

Salla Mattola ¹, Satu Hakanen ¹, Sami Salminen ¹, Vesa Aho ¹, Elina Mäntylä ², Teemu O. Ihalainen ², Michael Kann ^{3,4} and Maija Vihinen-Ranta ^{1,*}

¹ Department of Biological and Environmental Science, University of Jyväskylä, 40500 Jyväskylä, Finland; salla.m.mattola@jyu.fi (S.M.); satu.a.hakanen@jyu.fi (S.H.); sami.j.salminen@jyu.fi (S.S.); Vesa.p.aho@jyu.fi (V.A.)

² BioMediTech, Faculty of Medicine and Health Technology, Tampere University, 33520 Tampere, Finland; elina.mantyla@tuni.fi (E.M.); teemu.ihalainen@tuni.fi (T.O.I.)

³ Department of Infectious Diseases, Institute of Biomedicine, Sahlgrenska Academy, University of Gothenburg, 41390 Gothenburg, Sweden; michael.kann@gu.se

⁴ Department of Clinical Microbiology, Sahlgrenska University Hospital, 41345 Gothenburg, Sweden

* Correspondence: maija.vihinen-ranta@jyu.fi

Abstract: Parvoviruses are small single-stranded (ss) DNA viruses, which replicate in the nucleoplasm and affect both the structure and function of the nucleus. The nuclear stage of the parvovirus life cycle starts at the nuclear entry of incoming capsids and culminates in the successful passage of progeny capsids out of the nucleus. In this review, we will present past, current, and future microscopy and biochemical techniques and demonstrate their potential in revealing the dynamics and molecular interactions in the intranuclear processes of parvovirus infection. In particular, a number of advanced techniques will be presented for the detection of infection-induced changes, such as DNA modification and damage, as well as protein–chromatin interactions.

Keywords: parvoviruses; nucleus; imaging of viral interactions and dynamics; analysis of protein–protein interactions; analysis of virus–chromatin interactions



Citation: Mattola, S.; Hakanen, S.; Salminen, S.; Aho, V.; Mäntylä, E.; Ihalainen, T.O.; Kann, M.; Vihinen-Ranta, M. Concepts to Reveal Parvovirus–Nucleus Interactions. *Viruses* **2021**, *13*, 1306. <https://doi.org/10.3390/v13071306>

Academic Editor: Giorgio Gallinella

Received: 1 June 2021

Accepted: 2 July 2021

Published: 5 July 2021

Publisher's Note: MDPI stays neutral with regard to jurisdictional claims in published maps and institutional affiliations.



Copyright: © 2021 by the authors. Licensee MDPI, Basel, Switzerland. This article is an open access article distributed under the terms and conditions of the Creative Commons Attribution (CC BY) license (<https://creativecommons.org/licenses/by/4.0/>).

1. Introduction

Parvoviruses are not only significant pathogens causing diseases in humans and animals but also promising candidates in gene therapy, in oncolytic therapy, in vaccine development, and as passive immunization vectors [1–7]. Compared to some other viruses that only need a few viral particles for infection, parvoviruses are extremely inefficient. In infection and disease development, this incapability is compensated by high replication. Finding new ways to treat parvoviral diseases and to facilitate the development of parvovirus-based therapies requires deepening the understanding of infection and propagation in their host cells.

Although parvoviruses and their infection have been extensively studied throughout the past decades, there is still a lack of molecular level understanding of the virus–host cell interactions. Due to their low particles to infectious unit ratio, the identification and tracking of virus-induced events, which contribute to viral propagation, is a key challenge. Furthermore, the small size of parvovirus (~20 nm in diameter) hinders the attachment of fluorescent probes, which limits capsid detection by single-virus tracking.

Parvoviruses are divided into two classes: autonomous parvoviruses, such as canine parvovirus (CPV), minute virus of mice (MVM), and rat parvovirus (H-1PV), and dependoparvoviruses, such as adeno-associated viruses (AAV), which require coinfection with either adenoviruses or herpes simplex virus in their late stages of infection [8]. Parvoviruses are composed of two to three capsid proteins (viral proteins, VPs; VP1, 2, and 3). They enclose a c. 5 kb-long ssDNA genome, which consists of two overlapping open reading frames. The expression is controlled by two promoters, the early P4 and late P38. The former guides the expression of viral nonstructural proteins 1 and 2 (NS1 and

NS2), while the latter controls the expression of capsid proteins [9–11]. In the infectious virion, which has a diameter of 18–26 nm, the genome is covalently bound to the NS1 (Rep78 in AAV) protein [12–15]. This protein is cytotoxic and has central roles in viral replication attributed to its helicase, endonuclease, ATPase, and site-specific DNA-binding activities [16,17]. NS2 plays a role in viral replication [12,18], development of viral replication centres [19], viral mRNA translation [20], and the assembly [21] and nuclear egress of capsids [22–26]. In gene therapy, which is mostly based on AAV, the single-stranded genome is replaced by a double-stranded self-complementary genome, which does not allow replication [15].

After the cellular entry and cytoplasmic release, parvoviral capsids enter the nucleus through the nuclear pore complexes (NPCs) and/or via disruption of the nuclear envelope (NE) [27–34]. The VP1 capsid protein bears nuclear localization signals (NLSs) within its VP1-unique region in the N-terminal domain [35–41], which are thought to allow nuclear import by interaction with nuclear transport factors of the importin family [30,42,43]. In assembled capsids, this domain is hidden.

Once arriving in the nucleus, the genome replicates via a rolling circle mechanism, during which the genome concatemer is cleaved to monomers by NS1 [44]. The gene expression of parvoviruses is coupled to the S-phase of the cell cycle, and it leads to the formation of distinct replication centre foci where viral gene transcription and productive replication occur [19,45,46]. As the infection proceeds, the replication centres expand [27,28,47], which is accompanied by changes in the cellular chromatin structure and chromatin marginalization to the nuclear periphery at later stages of infection [45,47]. Besides the dramatic morphological changes, parvovirus infections are known to induce substantial damage to the host DNA [48–50], and MVM replication centres have been shown to associate with the sites of cellular DNA damage [51,52]. This allows the virus to recruit cellular DNA replication and DNA damage response proteins, which promote viral replication and gene expression [45,49,53]. NS1 of MVM is responsible for nicking the host DNA, which subsequently results in S phase cell cycle arrest [54]. However, during human parvovirus B19 (B19V) infection, a G2/M arrest is induced by the NS1 protein through a p53-independent pathway, which does not depend on the DNA damage response [50]. In addition to evoking disturbances in the cell cycle, parvoviruses are known to cause apoptosis of the infected cells, another hallmark of DNA damage [55,56].

These nuclear changes are followed by progeny capsid assembly in the nucleus, which is combined with the encapsidation of viral genomes covalently bound to NS1. The progeny virions leave the cell by lysis, probably after export from the nucleus [57–60]. This lytic viral release, in conjunction with the S-phase-dependent replication, enables the use of autonomous parvoviruses in oncotherapy for the destruction of rapidly dividing cancer cells [61].

2. Imaging of Viral Interactions and Dynamics in the Cytoplasm and Nucleus

To date, a broad variety of microscopy-based imaging and spectroscopy applications have enlightened the steps in the early infection of several parvoviruses (Figure 1). Upon nuclear import, CPV can pass the NE [27,28,62,63], which was confirmed by single-particle tracking analyses of fluorophore-labelled AAV capsids (Figure 1, boxes 1 and 2) [64]. Similar analyses have also been used to study the receptor binding of canine parvovirus [65,66] as well as the cytoplasmic trafficking [67] and nuclear import of AAV [27,28,64,68].

The schematic represents the fluorescent microscopy methodology for the imaging of the parvoviral life cycle in the nuclear region. (1) Analysis of fluorescent virus particle dynamics by single-particle tracking and high-speed super-resolution microscopy verified the import of viral capsids through the nuclear pore complex. Image correlation analysis using the pair correlation function (pCF) revealed the importin β -mediated nuclear transport of capsids. Confocal microscopy combined with EM characterized an alternative nuclear entry pathway for parvoviruses through virus-induced nuclear envelope ruptures. (2) Tracking of fluorescent capsids after their nuclear entry demonstrated that

they moved by diffusion in the nucleoplasm. Furthermore, image correlation using the autocorrelation function (ACF) indicated that the capsids were disintegrated after their nuclear import. (3) Super-resolution microscopy analysis indicated that viral replication centres were located close to sites of cellular DNA damage. Fluorescence recovery after photobleaching (FRAP) studies showed that infection affected the diffusion of nuclear proteins, such as transcription-associated proteins. (4) Fluorescent tagging of progeny capsids (green) has allowed for analyses of capsid dynamics in living cells. Images were created with BioRender.com.

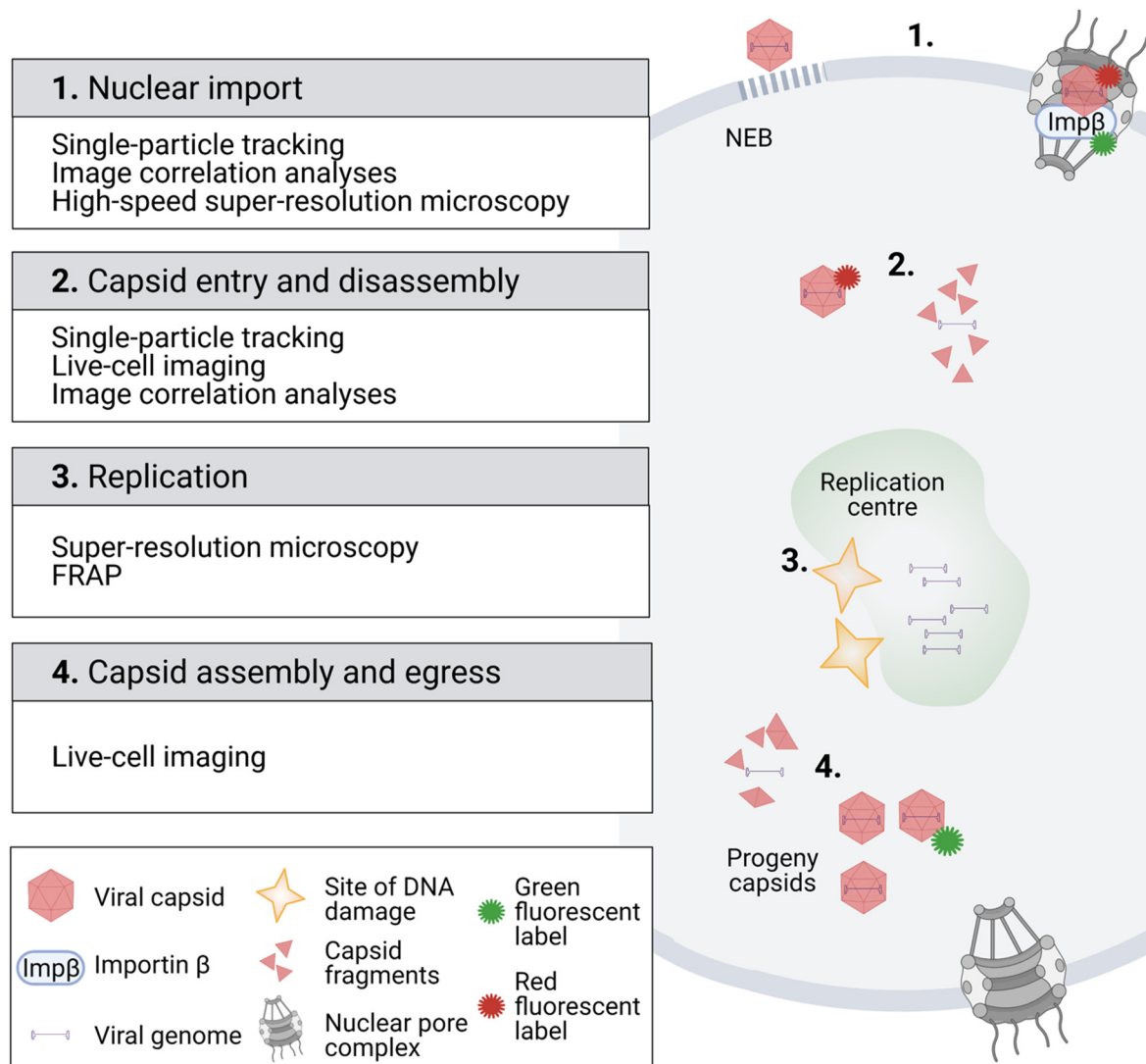


Figure 1. Imaging of viruses in the nucleus of infected cells.

Imaging of autonomous parvovirus capsids has partially been hampered by the limited possibilities to express recombinant viruses that contain fluorescent proteins, as the enlarged genome size leads to poor viral genome packaging. Therefore, little is known about virus–nucleus interactions following the assembly of viral capsid. However, AAV-2 studies have shown that large peptides can be inserted into the VP2 protein with a minimal effect on viral assembly or infectivity [69]. This has allowed the creation of fluorescent protein-tagged AAV particles for live cell analysis of intranuclear dynamics [70]. The loop regions of AAV capsid proteins exposed to the capsid surface have been used for the insertion of shorter peptides, which enables the labelling of viral particles with a fluorescent dye [71,72].

Tracking of individual viruses is a powerful tool to examine the mechanisms of their intracellular transport, and it is straightforward, for example, to conclude whether the motion is directed or random diffusion. For active processes, such as transport along microtubules, the dynamics can be deduced from a low number of particles. However, insight into the parvoviral life cycle has revealed the diffusive dynamics of events. For example, following of the trajectories of Cy5-labelled AAV capsids in the cytoplasm and nucleus showed that the majority of capsids move by regular diffusion, but a smaller fraction of the capsids exhibits anomalous subdiffusion [64]. The analysis of a small number of randomly moving diffusing particles is challenging, but when the motions of typically hundreds or thousands of particles are averaged, their movement can be characterized. The mean squared displacement (MSD) of the particles follows the law $MSD = 2dDt$, where D is the diffusion coefficient of the particle, d is the dimensionality of the motion, and t is the time. Measuring the MSD allows for the determination of the particle diffusion coefficient, which can then be further connected to the particle radius r , temperature T , and viscosity η of the medium by the Stokes–Einstein equation:

$$D = \frac{k_B T}{6\pi\eta r}.$$

Recently, image correlation spectroscopy has been used to verify the nuclear capsid import and intranuclear disassembly of capsids in living cells (Figure 1, boxes 1 and 2) [30]. Image correlation methods are based on the principles of fluorescence correlation spectroscopy (FCS), which measures fluctuations of fluorescence intensity in a small volume by using the focused excitation laser beam. The recorded fluctuations in photon counts, collected as a time series, are used to calculate the time autocorrelation function (ACF) to resolve the dynamics of fluorescently tagged proteins. The ACF represents the correlation of the fluorescent signal between the starting time point ($t = t_0$) and following time points ($t = t_0 + \Delta t$) of the experiment, thus yielding information on fluorescent molecule diffusion time in the focal spot. In parvovirus studies, the ACF calculated for a time series of laser scanning microscopy images containing temporal information of the intensity fluctuations and spatial distribution maps of the fluorescent viral particles has enabled the analysis of fast and slow diffusion, or even immobile viral particles [30].

To obtain more information about the possible directed movement of fluorescent particles, pair correlation function (pCF) analysis can also be used. The pCF measures the correlation over time and space and thus can distinguish directed movement or obstacles to diffusion. In parvovirus studies, pCF revealed a positive correlation between pixels across the NE within an image series, thereby demonstrating the nuclear import of capsid through the NE [30,73–75]. In addition, pCF analysis detected a spatiotemporal correlation between the fluorescent viral capsid and importin β , suggesting that importin β mediates capsid translocation through the nuclear pore complex [30]. An alternative or parallel existing nuclear entry pathway has been derived from studies using fluorescence and electron microscopy. The experiments have demonstrated that the NE undergoes substantial damage at early times during parvovirus H1, CPV, and AAV2 infection, indicating an NPC-independent nuclear entry of capsids [31,33].

The theoretical nuclear diffusion coefficient of capsids obtained from the Stokes–Einstein law, assuming that the viscosity of the nucleoplasm is approximately four times higher than in water [76,77], is in the order of $10 \mu\text{m}^2/\text{s}$. This is in accordance with the experimental finding of $5 \mu\text{m}^2/\text{s}$ obtained for the mobile population of virus-like particles of parvovirus [30,47]. In the cellular scale, this is a relatively fast diffusion rate, and it means that on average, the virus particles are able to diffuse a $10 \mu\text{m}$ distance in a time scale of a few seconds, when not restricted by physical barriers or by interactions.

Studies of nucleoplasmic capsid diffusion coefficients by ACF, which improved temporal resolution from the millisecond to microsecond scale, have revealed distinct diffusion dynamics for intact capsids and potential capsid fragments, suggesting that capsids are disintegrated in the nucleoplasm after their import [30]. The detailed mechanisms by which

the viral genome is released into the nucleoplasm remain to be determined. However, fluorescence microscopy analyses have shown that capsids are already modified prior to nuclear import and nuclear disassembly when VP1 N-terminus is exposed during the endocytic entry [41,78–80]. According to immunoprecipitation analyses, B19V capsid uncoating is enhanced by cytoplasmic divalent cations [81]. Previously published studies have demonstrated that at least for MVM, the nuclear release of DNA occurs without a complete disassembly of the capsids [78,82–85]. In summary, it can be concluded that parvoviral capsids enter the nucleus either via NPC or by passing through transient holes in the NE, which allow the entry of intact capsids. Intact capsids entering the nucleus may undergo structural change which leads to viral genome release at some distance from the NE [30,86].

As outlined before, progressing parvovirus infection leads to the development of viral replication centres [46,87] and relocation of host chromatin to the nuclear periphery [45,47–49,88]. Recently, super-resolution microscopy has demonstrated that viral replication centres originate close to DNA damage sites (Figure 1, box 3) [52]. The introduction of photobleaching experiments in the analyses of intranuclear mobility and kinetics of viral and cellular proteins has allowed a better monitoring of nuclear changes upon parvoviral infection (Figure 1, box 3). In these studies, a high-intensity laser is used to photobleach the fluorescence of a fluorescent molecule, typically a fluorescent fusion protein, from a defined area of the cell. In fluorescence recovery, after photobleaching (FRAP), a region of interest is bleached, and the recovery of fluorescence in the bleached region is measured. The rate of fluorescence recovery is determined by the exchange of fluorescent molecules between the bleached region and the surrounding unbleached area, thereby allowing the analysis of protein dynamics and interactions. In fluorescence loss in photobleaching (FLIP), an area of the cell is continuously photobleached with laser pulses, and images taken between the pulses measure the response in the entire pool of fluorescent molecules. Similar to FRAP, the rate of fluorescence loss is related to the mobility of the fluorescent molecules.

In CPV infection, FRAP experiments (Figure 1, box 3) have revealed that the dynamics of transcription-associated protein change during infection [89] and further demonstrated that infection leads to an increased protein mobility in the nucleoplasm, which potentially alters protein–protein and protein–DNA binding reactions during viral replication [47]. Additionally, FRAP has been used to study the kinetics of NS1-EYFP in noninfected cell nuclei. The results have shown that NS1-EYFP mobility is not consistent with free diffusion and suggested transient binding to nuclear components [90]. Shown by FLIP, the nucleocytoplasmic shuttling of NS1-EYFP has been discovered [90].

Further central questions in the late stages of the nuclear life cycle of parvoviruses, such as capsid assembly and nuclear egress, have been addressed using fluorescent microscopy of immunostained cells. These studies, in combination with biochemical characterizations, showed that MVM capsids assemble in the nucleus from VP1/VP2 trimers [60,91], and these trimers expose a structured nuclear localization motif [58]. For AAV-2, the subcellular localization of capsid assembly to nucleoli was identified with immunofluorescence and in situ hybridization microscopy techniques. Viral genome sequence analysis and mutational studies revealed that the capsid assembly is mediated by the viral assembly associated protein (AAP) [92,93]. Moreover, X-ray crystallography and cryo-EM analyses of MVM capsids demonstrated that viral DNA is packed through a fivefold packaging channel [94,95]. Studies have also revealed that MVM capsids leave the nucleus prior to cell lysis and NE breakdown [96], suggesting that capsids have to exit the nucleus through the NPCs [22,23]. A similar combination of techniques was used to show that MVM capsids egress the nucleus dependent upon chromosomal region maintenance 1 (CRM1, also known as exportin 1) protein [96], which is a nuclear export factor for various proteins and different cellular RNAs (snRNA, rRNA, some mRNAs) [97]. Notably, the nuclear exit was limited to genome-containing capsids phosphorylated in the unordered domain of VP2, while empty capsids exhibited nuclear accumulation [96]. By combining classical immunofluorescence microscopy with surface plasmon resonance spectroscopy,

it has been shown that the CRM1-dependent nuclear export of MVM capsids is mediated by the supraphysiological NES in NS2 [22].

3. Screening and Validation of Protein–Protein Interactions

The nuclear import of intact parvovirus capsids is not limited by the NPC diameter, which is able to transport particles with a diameter of ~39 nm [98]. There is accumulating evidence that the nuclear entry of the parvovirus capsid depends on the host machinery for nuclear import, requiring coordinated interaction with different host proteins. Earlier studies have shown that the capsid proteins of MVM and CPV, in addition to AAV capsids, have basic regions containing NLSs or a structured nuclear localization motif in their capsid proteins. [35–41,60,79] During endocytic entry, the acidification of capsid leads to NLS exposure, and after reaching the cytoplasm, this would thus allow the attachment of nuclear import factors. Studies including coimmunoprecipitation assays (Co-IP) have verified that CPV and AAV2 capsids interact with Imp β [42,99]. However, these assays elucidate neither the localization of the interaction in the cell environment nor the phase of the infection. The proximity ligation assay (PLA) has allowed comprehensive imaging and quantitation of interactions within the host cell. This antibody-based technique enables the detection of two proteins that are in close proximity to each other (~40 nm) [100]. Therefore, PLA is capable of visualizing protein–protein interactions beyond the diffraction limit (Figure 2A). For CPV, in situ proximity ligation analysis, combined with confocal microscopy and image analysis, has demonstrated that capsids are able to recruit cytoplasmic Imp β for nuclear transport [42]. Coimmunoprecipitation analyses have indicated that entering H-1PV and AAV2 capsids interact with nucleoporins, which are proteins of the NPC [31].

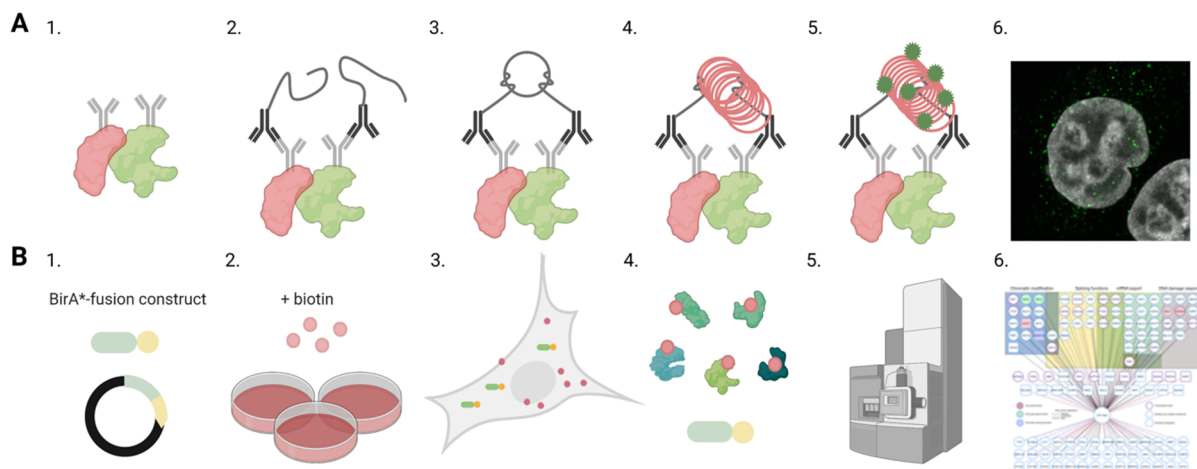


Figure 2. Analyses of protein–protein interactions in infection. Schematic overviews of proximity ligation assay (PLA) and proximity-dependent biotin identification (BioID) methods to identify and localize interactions between viral and host proteins. **(A)** The schematic representation of PLA assay. (1) Primary antibodies are used to target proteins of interest shown in red and green. (2) Secondary antibodies with PLA oligonucleotide probes bind to the primary antibodies. (3) Closely located PLA probes are ligated together, and (4) the formed circular DNA is amplified. (5) The amplified DNA (red) is labelled by fluorescent probes (green). (6) Confocal microscopy image shows the intracellular distribution of the PLA signals (green). Nuclei were stained with DAPI (grey). **(B)** Outlines of the BioID workflow. (1) Transfection of cells with BirA*-viral protein-fusion constructs and the generation of a stable inducible cell line. (2) Addition of biotin to the culture media and viruses if infection is required. (3) Cell culture period during which biotin ligase activity of BirA* fusion protein induces proximity-dependent biotinylation of neighbouring endogenous and viral proteins. (4) Cell lysis and the streptavidin-affinity purification of biotinylated proteins from cell lysates. (5) Mass spectrometry and analyses of protein associations. (6) Interaction network indicating interaction partners of viral protein and biological processes involved. Images were created with BioRender.com.

Knowledge of viral protein interactions with cellular proteins is essential for understanding the intranuclear processes such as viral replication, capsid assembly, and nuclear egress. Affinity purification-mass spectrometry proteomics approaches have been traditionally used to analyse protein–protein interactions in infection [101–103]. Recently, many new screening methods have been generated to recognize protein–protein associations [104–106]. One of the methods is the proximity-dependent biotin identification (BioID) assay combined with mass spectrometry [107–109] (Figure 2B). BioID is a proximity-tagging method that utilizes a fusion of promiscuous biotin ligase, BirA, to a protein of interest to identify protein–protein associations and proximate proteins. The working radius for biotinylation via BirA is 10–40 nm, depending on the used application. Mass spectrometry-based proteomics applications such as BioID are able to recognize highly transient protein–protein interactions during the viral lifecycle. BioID studies of parvovirus human bocavirus 1 (HBoV1) have revealed interaction between viral nuclear protein 1 (NP1) and factors mediating nuclear import and mRNA processing [110]. A BioID analysis of AAV2 Rep proteins has revealed their association with cellular proteins, such as the transcriptional corepressor KAP1, which assist the viral genome in resisting epigenetic silencing, thereby allowing the lytic replication of AAV [111]. BioID has also been used to recognize interactions between viral proteins and DNA damage-related proteins. BioID has revealed an AAV Rep protein interaction with the Mre11 part of the MRN complex, an important initiator of the AMT response [111]. Overall, BioID has allowed for identifying associations of the viral protein of interest in a wide variety of nuclear processes, which, for CPV NS2, include DNA damage response and chromatin modification [112].

4. Detection of DNA Damage, DNA Repair, and Virus–DNA Interactions

Progression of parvovirus infection depends upon the induction of a cell cycle arrest and cell lysis. It leads to the activation of DNA damage response (DDR) [19,45], which promotes the infection and viral reproduction [113,114]. Ataxia telangiectasia and Rad3(ATR)-mediated DDR activation is linked to replication fork stalling, whereas the activation of the Ataxia-telangiectasia mutated (ATM)-mediated route is the initial response to a double-stranded DNA break (DSB) [115,116]. The activation of the ATR route has been observed for MVM, B19, and HBoV1 [51,111,112], and the ATM route for MVM, HBoV1, and AAV [45,117–119] (Figure 3A). Recognition of DNA damage induces the recruitment of proteins responsible for DNA damage repair to the site of the damage. During parvovirus infection, the emergence of DNA damage can be observed either indirectly by the accumulation of DDR proteins to the damage site or by observing the formation of actual DNA breakages. MVM infection has been shown to cause accumulation of proteins of the ATM signalling route (e.g., phosphorylated H2AX (γ -H2AX), Nbs1, RPA32, Chk2, p53, MDC1, MRN) to the replication start sites together with the viral replication protein NS1 [19,45]. During viral replication, at least newly synthesized viral DNA is bound to RPA, a known activator of ATR [120]. However, in MVM infection, this does not lead to the full activation of the ATR response since checkpoint kinase1 (Chk1) is not activated [49,51] (Figure 3A).

Recently, a high-throughput viral chromosome conformation capture sequencing assay (V3C-seq) has been applied to study the association of MVM viral genomes with host chromatin [121] (Figure 3C). V3C-seq is based on the chromosome conformation capture sequencing technology (3C-seq) [122] used to study chromosome arrangement in the nucleus by crosslinking the sites of genomic associations and identifying these regions with sequencing. 3C-seq studies have revealed that MVM genomes become associated with DNA damage sites during early stages of infection [121]. These sites of DNA damage with associated viral genomes increase as the infection proceeds. Nuclear localization of this association was further verified with fluorescent in situ hybridization (FISH) and super-resolution stochastic optical reconstruction microscopy (STORM). The introduction of externally induced DNA damage sites with laser irradiation or with CRISPR-Cas9 to a specific genomic locus resulted in parvoviral genome association with these regions. V3C-seq analyses have also revealed that the viral genome association sites and DNA

damage sites overlap with self-interacting genetic regions, also known as topologically associating domains (TADs) [52]. Recently, it has been shown that the localization of viral genomes to the DNA damage sites is mediated by viral NS1 [121].

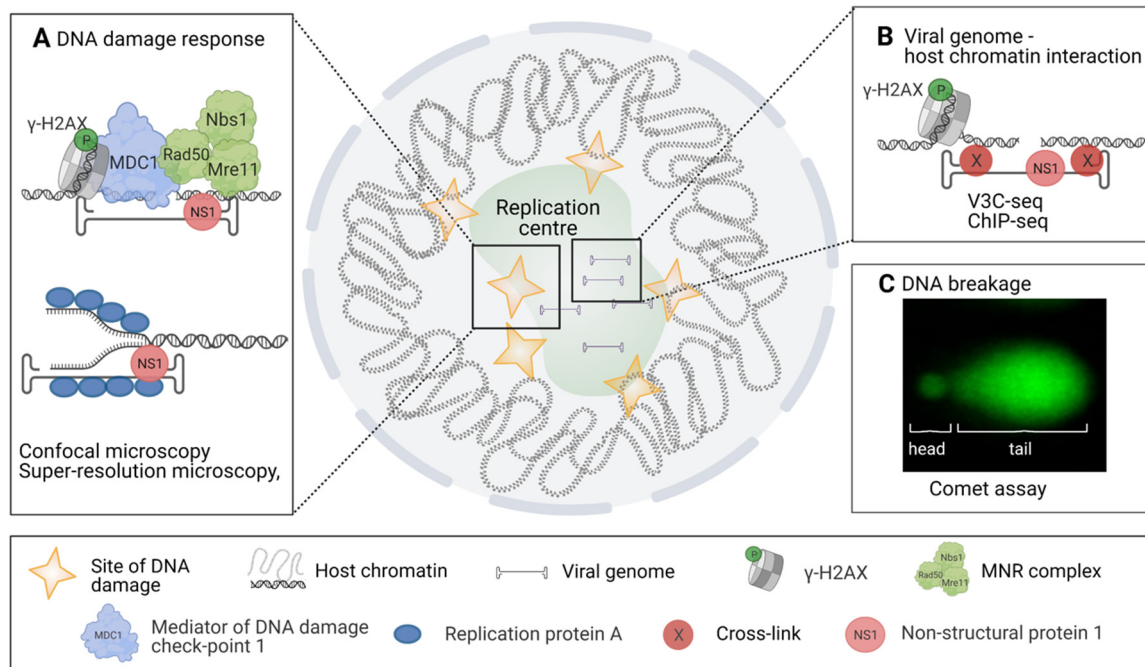


Figure 3. Approaches revealing virus-induced DNA damage. The schematic diagram of diverse methods for the analyses of DNA damage response (DDR), viral and host DNA interactions, and DNA damage in infection. **(A)** Analyses of ATM and ATR-mediated DNA damage signalling pathways by confocal and super-resolution microscopy, ATM-mediated cellular response to DNA damage functions through phosphorylation of proteins related to DNA damage and DNA damage repair such as γ -H2AX, MDC1, Rad50, Nbs1, and Mre11. In MVM infection these proteins are found in replication start sites together with viral NS1. In parvovirus-infected cells, the ATR-mediated response depends on RPA and viral NS1 interaction. **(B)** Elucidation of interactions between viral genome and host cell chromatin by using high-throughput viral chromosome conformation capture sequencing assay (V3C-seq). Moreover, association of DNA damage site MVM genomes has been shown by ChIP-seq. This analysis has been used to verify the association between NS1-mediated viral genome replication and DDR. **(C)** Studies of host cell chromatin disintegration by comet assay. Images were created with BioRender.com.

Classical DNA damage analyses in viral infection are qPCR or agarose gel electrophoresis, which do not allow investigations on the single-cell level. This obstacle was solved by comet assay—also known as single-cell gel electrophoresis—which is a sensitive, quantitative, and relatively simple imaging-based method to observe DNA breakages (Figure 3C) [123–125]. Scraped or trypsinized cells are cast into low-density agarose gel and lysed, after which the remaining nucleoids are placed in an electric field and stained. DNA lesions, both single and double stranded, result in a relaxation of DNA supercoiling. The relaxed DNA loops migrate towards the positively charged pole during electrophoresis, forming the characteristic comet tail pattern. The relative DNA content in the comet tail versus the head thus reflects the number of DNA lesions. Unlike the various DDR pathway markers, which might be activated in response to viral genomes or proteins [126], this method relies on the physical properties of damaged host DNA. Comet assay studies and ChIP-seq analysis have demonstrated that MVM infection causes host DNA damage, which increases as the infection proceeds [52]. In contrast, the comet assay has revealed no significant DNA damage in cells infected by the bocavirus minute virus of canine [127], nor in cells infected by human B19V [127]. The potential nucleolytic activity of parvoviral NS1 protein against host DNA has been investigated in expression studies for HBoV1 [117]

and human B19V [127], but these studies did not find significant host DNA damage in NS1-expressing cells.

To benefit from host cell responses such as the DDR, viral proteins or viral genomes are required to interact directly with DNA or DNA-modifying proteins. The interactions of cellular DNA-binding proteins and viral proteins with host chromatin and viral genomes in MVM and CPV infections have been studied by ChIP-seq methods [52,88,121]. These studies have shown the acetylation of histones bound to CPV genome and MVM genome association with cellular γ -H2AX sites and the viral NS1 protein [52,88,121] (Figure 3B). Furthermore, the studies of the genomic reactivation of latent AAV genome by ChIP and ChIP coupled to qPCR have revealed the mechanism by which cellular proteins induce viral genome repression [111].

5. Recent Methods for Future Studies of Parvovirus–Nucleus Interactions

Despite of decades of research, many detailed mechanisms of virus–host interactions are not well understood, and many new observations raise further questions, requiring the use of newly developed techniques. Next-generation sequencing (NGS) and fluorescence imaging technologies are currently advancing rapidly [128,129], offering excellent opportunities for detailed analysis of infection-induced changes in the host chromatin organization and high-resolution imaging of parvovirus infection. For example, these methods combined with spatial transcriptomics allow analyses of the spatial heterogeneity of the gene expression within the sample [130–133].

NGS is a modern sequencing methodology where massive parallel sequencing is used to map the sequences of millions of small DNA fragments. Bioinformatics is then used to combine the acquired sequencing data, which can be then compared to reference genome(s). Various approaches allow for obtaining information about expressed genes [134], genome accessibility [135], binding regions of different DNA interacting proteins [136–138], or chromatin–chromatin interactions and organization [139]. As an example, the assay for transposase-accessible chromatin with sequencing (ATAC-seq) is based on hyperactive Tn5 transposase mutants [135]. In this assay, the hyperactive Tn5 is used to tagment the accessible chromatin by conjugating short and specific DNA oligomers into the accessible regions. These regions of the genome are then isolated and sequenced, yielding a high-resolution map of the accessible regions of the genome. Thus, ATAC-seq has great potential in studies on how parvoviral infection changes the host cell chromatin organization or in studies of viral genome packaging or release. This is exemplified by recent results showing that baculovirus infection induces significant changes in the organization of host genome, such as an increase in chromatin accessibility, relocation close to the NE, and nucleosome disassembly [140]. Moreover, ATAC-seq analysis of Epstein–Barr virus (EBV), a member of the herpesvirus family, has demonstrated that B cell chromatin undergoes significant remodelling during infection, which leads to the regulation of cell cycle, apoptosis pathways, and interferon regulatory factors [141]. Another example of a similar DNA-tagging method is DNA adenine methyltransferase identification (DamID)-sequencing [142]. Here, DNA adenine methyltransferase (Dam) is fused to a protein of interest, and this fusion protein is expressed in cells. The Dam enzyme recognizes DNA sequence GATC and methylates the adenine in the close vicinity of the fusion protein. These methylated regions of chromatin can then be sequenced and mapped. Thus, these sequences correspond to the chromatin that has been in close vicinity to the expressed fusion protein. This DamID-seq has been used to map the chromatin interacting with the nuclear lamina and lamina-associated domains [143]. In addition to sequencing, both ATAC-seq and DamID-seq can be combined with high-resolution fluorescence imaging. In the case of ATAC-seq, fluorescent oligomers are used together with hyperactive Tn5, and therefore, the tagmented and accessible chromatin can be visualized by fluorescence microscopy. This ATAC-seq method [144] allows imaging the accessible chromatin regions and would be directly applicable to parvoviral studies regarding host cell chromatin or viral genome organization. DamID can be used together with methylated DNA-recognizing fluorescent ^{m6}A-tracer fusion protein.

^{m6}A-tracer binds to the GATC sequence when adenine is methylated by Dam methylase. By fusing ^{m6}A-tracer to a fluorescent protein, the fluorescent signal localizes to the methylated DNA [145]. The great advantage of the DamID ^{m6}A-tracer system is the possibility to use it in living cells. Thus, one can follow the chromatin dynamics by live cell microscopy. We envision that the system could be used to follow parvovirus infection-induced dynamic reorganization of the host genome.

Imaging and sequencing approaches are directly combined in spatial transcriptomics, where transcriptomes are resolved by high resolution microscopy or by capturing, so that spatial information about the location is also recorded. In microscopy-based spatially resolved transcriptomics or genomics, the different RNA and DNA species are labelled via sequential fluorescence in situ hybridization and barcoding. This approach offers the highest resolution, and recently, the imaging of 3660 chromosomal loci together with 17 chromatin marks in single cells has been reported [146].

6. Concluding Remarks

Conventional confocal microscopy approaches, including the imaging of fluorescent viral capsids and proteins and their interplay with cellular components within the host cell, have been successfully used in parvovirus studies. The development of live cell imaging and super-resolution microscopy, combined with image data analysis, together with the development of new screening tools for analyses of protein–protein and DNA–protein interactions, has further enhanced our understanding of virus–nucleus interactions and the nuclear dynamics of infection. In the near future, combining fluorescence data and ultrastructural information from electron micrographs will allow answering detailed questions regarding the mechanisms of intranuclear events in viral infection. Moreover, the advances in super-resolution microscopy applications will enable us to probe cell–virus interactions and dynamics in previously unattainable detail.

Author Contributions: S.M., S.H., S.S., V.A., E.M., T.O.I., M.K. and M.V.-R. wrote the paper. All authors have read and agreed to the published version of the manuscript.

Funding: This research was funded by the Jane and Aatos Erkko Foundation (M.V.-R.), Academy of Finland, grant numbers n330896 (M.V.-R.), 308315 (T.O.I.), 314106 (T.O.I.), and 332615 (E.M.); the Biocenter Finland, viral gene transfer (M.V.-R.); the Graduate School of the University of Jyväskylä (S.M.); and a starting grant of the University of Gothenburg (M.K.).

Institutional Review Board Statement: Not applicable.

Informed Consent Statement: Not applicable.

Data Availability Statement: Data available in a publicly accessible repository.

Conflicts of Interest: The authors declare no conflict of interest.

References

1. Heegaard, E.D.; Brown, K.E. Human Parvovirus B19. *Clin. Microbiol. Rev.* **2002**, *15*, 485–505. [[CrossRef](#)] [[PubMed](#)]
2. Nandi, S.; Kumar, M. Canine Parvovirus: Current Perspective. *Indian J. Virol.* **2010**, *21*, 31–44. [[CrossRef](#)] [[PubMed](#)]
3. Kotterman, M.A.; Schaffer, D.V. Engineering Adeno-Associated Viruses for Clinical Gene Therapy. *Nat. Rev. Genet.* **2014**, *15*, 445–451. [[CrossRef](#)] [[PubMed](#)]
4. Li, C.; Samulski, R.J. Engineering Adeno-Associated Virus Vectors for Gene Therapy. *Nat. Rev. Genet.* **2020**, *21*, 255–272. [[CrossRef](#)] [[PubMed](#)]
5. Marchini, A.; Bonifati, S.; Scott, E.M.; Angelova, A.L.; Rommelaere, J. Oncolytic Parvoviruses: From Basic Virology to Clinical Applications. *Viol. J.* **2015**, *12*, 1–16. [[CrossRef](#)]
6. Zabaleta, N.; Dai, W.; Bhatt, U.; Chichester, J.A.; Estelien, R.; Sanmiguel, J.; Michalson, K.T.; Diop, C.; Maciorowski, D.; Qi, W.; et al. Immunogenicity of an AAV-Based, Room-Temperature Stable, Single Dose COVID-19 Vaccine in Mice and Non-Human Primates. *bioRxiv* **2021**. [[CrossRef](#)]
7. Tse, L.V.; Meganck, R.M.; Graham, R.L.; Baric, R.S. The Current and Future State of Vaccines, Antivirals and Gene Therapies Against Emerging Coronaviruses. *Front. Microbiol.* **2020**, *11*, 658. [[CrossRef](#)]

8. Péntzes, J.J.; Söderlund-Venermo, M.; Canuti, M.; Eis-Hübinger, A.M.; Hughes, J.; Cotmore, S.F.; Harrach, B. Reorganizing the Family Parvoviridae: A Revised Taxonomy Independent of the Canonical Approach Based on Host Association. *Arch. Virol.* **2020**, *165*, 2133–2146. [[CrossRef](#)]
9. Cotmore, S.F.; Tattersall, P. Dna Replication in the Autonomous Parvoviruses. *Semin. Virol.* **1995**, *6*, 271–281. [[CrossRef](#)]
10. Li, X.; Rhode, S.L. Mutation of Lysine 405 to Serine in the Parvovirus H-1 NS1 Abolishes Its Functions for Viral DNA Replication, Late Promoter Trans Activation, and Cytotoxicity. *J. Virol.* **1990**, *64*, 4654–4660. [[CrossRef](#)]
11. Christensen, J.; Cotmore, S.F.; Tattersall, P. Minute Virus of Mice Transcriptional Activator Protein NS1 Binds Directly to the Transactivation Region of the Viral P38 Promoter in a Strictly ATP-Dependent Manner. *J. Virol.* **1995**, *69*, 5422–5430. [[CrossRef](#)]
12. Naeger, L.K.; Cater, J.; Pintel, D.J. The Small Nonstructural Protein (NS2) of the Parvovirus Minute Virus of Mice Is Required for Efficient DNA Replication and Infectious Virus Production in a Cell-Type-Specific Manner. *J. Virol.* **1990**, *64*, 6166–6175. [[CrossRef](#)] [[PubMed](#)]
13. Tullis, G.E.; Labieniec-Pintel, L.; Clemens, K.E.; Pintel, D. Generation and Characterization of a Temperature-Sensitive Mutation in the NS-1 Gene of the Autonomous Parvovirus Minute Virus of Mice. *J. Virol.* **1988**, *62*, 2736–2744. [[CrossRef](#)]
14. Cotmore, S.F.; Gottlieb, R.L.; Tattersall, P. Replication Initiator Protein NS1 of the Parvovirus Minute Virus of Mice Binds to Modular Divergent Sites Distributed throughout Duplex Viral DNA. *J. Virol.* **2007**, *81*, 13015–13027. [[CrossRef](#)]
15. McCarty, D.M.; Pereira, D.J.; Zolotukhin, I.; Zhou, X.; Ryan, J.H.; Muzyczka, N. Identification of Linear DNA Sequences That Specifically Bind the Adeno-Associated Virus Rep Protein. *J. Virol.* **1994**, *68*, 4988–4997. [[CrossRef](#)] [[PubMed](#)]
16. Niskanen, E.A.; Ihalainen, T.O.; Kallioliinna, O.; Häkkinen, M.M.; Vihinen-Ranta, M. Effect of ATP Binding and Hydrolysis on Dynamics of Canine Parvovirus NS1. *J. Virol.* **2010**, *84*, 5391–5403. [[CrossRef](#)]
17. Niskanen, E.A.; Kallioliinna, O.; Ihalainen, T.O.; Hakkinen, M.; Vihinen-Ranta, M. Mutations in DNA Binding and Transactivation Domains Affect the Dynamics of Parvovirus NS1 Protein. *J. Virol.* **2013**, *87*, 11762–11774. [[CrossRef](#)]
18. Brownstein, D.G.; Smith, A.L.; Johnson, E.A.; Pintel, D.J.; Naeger, L.K.; Tattersall, P. The Pathogenesis of Infection with Minute Virus of Mice Depends on Expression of the Small Nonstructural Protein NS2 and on the Genotype of the Allotropic Determinants VP1 and VP2. *J. Virol.* **1992**, *66*, 3118–3124. [[CrossRef](#)] [[PubMed](#)]
19. Ruiz, Z.; Mihaylov, I.S.; Cotmore, S.F.; Tattersall, P. Recruitment of DNA Replication and Damage Response Proteins to Viral Replication Centers during Infection with NS2 Mutants of Minute Virus of Mice (MVM). *Virology* **2011**, *410*, 375–384. [[CrossRef](#)] [[PubMed](#)]
20. Naeger, L.K.; Salomé, N.; Pintel, D.J. NS2 Is Required for Efficient Translation of Viral mRNA in Minute Virus of Mice-Infected Murine Cells. *J. Virol.* **1993**, *67*, 1034–1043. [[CrossRef](#)]
21. Cotmore, S.F.; D'Abramo, A.M.; Carbonell, L.F.; Bratton, J.; Tattersall, P. The NS2 Polypeptide of Parvovirus MVM Is Required for Capsid Assembly in Murine Cells. *Virology* **1997**, *231*, 267–280. [[CrossRef](#)]
22. Engelsma, D.; Valle, N.; Fish, A.; Salomé, N.; Almendral, J.M.; Fornerod, M. A Supraphysiological Nuclear Export Signal Is Required for Parvovirus Nuclear Export. *Mol. Biol. Cell* **2008**, *19*, 2544–2552. [[CrossRef](#)]
23. Eichwald, V.; Daeffler, L.; Klein, M.; Rommelaere, J.; Salomé, N. The NS2 Proteins of Parvovirus Minute Virus of Mice Are Required for Efficient Nuclear Egress of Progeny Virions in Mouse Cells. *J. Virol.* **2002**, *76*, 10307–10319. [[CrossRef](#)]
24. Miller, C.L.; Pintel, D.J. Interaction between Parvovirus NS2 Protein and Nuclear Export Factor Crm1 Is Important for Viral Egress from the Nucleus of Murine Cells. *J. Virol.* **2002**, *76*, 3257–3266. [[CrossRef](#)]
25. López-Bueno, A.; Valle, N.; Gallego, J.M.; Pérez, J.; Almendral, J.M. Enhanced Cytoplasmic Sequestration of the Nuclear Export Receptor CRM1 by NS2 Mutations Developed in the Host Regulates Parvovirus Fitness. *J. Virol.* **2004**, *78*, 10674–10684. [[CrossRef](#)]
26. Hashemi, H.; Condurat, A.L.; Stroh-Dege, A.; Weiss, N.; Geiss, C.; Pilet, J.; Bartolomé, C.C.; Rommelaere, J.; Salomé, N.; Dinsart, C. Mutations in the Non-Structural Protein-Coding Sequence of Protoparvovirus h-1pv Enhance the Fitness of the Virus and Show Key Benefits Regarding the Transduction Efficiency of Derived Vectors. *Viruses* **2018**, *10*, 150. [[CrossRef](#)]
27. Kelich, J.M.; Ma, J.; Dong, B.; Wang, Q.; Chin, M.; Magura, C.M.; Xiao, W.; Yang, W. Super-Resolution Imaging of Nuclear Import of Adeno-Associated Virus in Live Cells. *Mol. Ther. Methods Clin. Dev.* **2015**, *2*, 15047. [[CrossRef](#)]
28. Junod, S.L.; Saredy, J.; Yang, W. Nuclear Import of Adeno-Associated Viruses Imaged by High-Speed Single-Molecule Microscopy. *Viruses* **2021**, *13*, 167. [[CrossRef](#)]
29. Mäntylä, E.; Kann, M.; Vihinen-Ranta, M. Protoparvovirus Knocking at the Nuclear Door. *Viruses* **2017**, *9*, 286. [[CrossRef](#)]
30. Mäntylä, E.; Chacko, J.V.; Aho, V.; Parrish, C.R.; Shahin, V.; Kann, M.; Digman, M.A.; Gratton, E.; Vihinen-Ranta, M. Viral Highway to Nucleus Exposed by Image Correlation Analyses. *Sci. Rep.* **2018**, *8*, 1–11. [[CrossRef](#)]
31. Porwal, M.; Cohen, S.; Snoussi, K.; Popa-Wagner, R.; Anderson, F.; Dugot-Senant, N.; Wodrich, H.; Dinsart, C.; Kleinschmidt, J.A.; Panté, N.; et al. Parvoviruses Cause Nuclear Envelope Breakdown by Activating Key Enzymes of Mitosis. *PLoS Pathog.* **2013**, *9*, e1003671. [[CrossRef](#)]
32. Cohen, S.; Panté, N. Pushing the Envelope: Microinjection of Minute Virus of Mice into Xenopus Oocytes Causes Damage to the Nuclear Envelope. *J. Gen. Virol.* **2005**, *86*, 3243–3252. [[CrossRef](#)]
33. Cohen, S.; Behzad, A.R.; Carroll, J.B.; Panté, N. Parvoviral Nuclear Import: Bypassing the Host Nuclear-Transport Machinery. *J. Gen. Virol.* **2006**, *87*, 3209–3213. [[CrossRef](#)]
34. Ros, C.; Bayat, N.; Wolfisberg, R.; Almendral, J.M. Protoparvovirus Cell Entry. *Viruses* **2017**, *9*, 313. [[CrossRef](#)]

35. Lombardo, E.; Ramírez, J.C.; Garcia, J.; Almendral, J.M. Complementary Roles of Multiple Nuclear Targeting Signals in the Capsid Proteins of the Parvovirus Minute Virus of Mice during Assembly and Onset of Infection. *J. Virol.* **2002**, *76*, 7049–7059. [[CrossRef](#)]
36. Vihinen-Ranta, M.; Kakkola, L.; Kalela, A.; Vilja, P.; Vuento, M. Characterization of a Nuclear Localization Signal of Canine Parvovirus Capsid Proteins. *Eur. J. Biochem.* **1997**, *250*, 389–394. [[CrossRef](#)]
37. Vihinen-Ranta, M.; Wang, D.; Weichert, W.S.; Parrish, C.R. The VP1 N-Terminal Sequence of Canine Parvovirus Affects Nuclear Transport of Capsids and Efficient Cell Infection. *J. Virol.* **2002**, *76*, 1884–1891. [[CrossRef](#)]
38. Popa-Wagner, R.; Sonntag, F.; Schmidt, K.; King, J.; Kleinschmidt, J.A. Nuclear Translocation of Adeno-Associated Virus Type 2 Capsid Proteins for Virion Assembly. *J. Gen. Virol.* **2012**, *93*, 1887–1898. [[CrossRef](#)]
39. Liu, P.; Chen, S.; Wang, M.; Cheng, A. The Role of Nuclear Localization Signal in Parvovirus Life Cycle. *Virol. J.* **2017**, *14*, 1–6. [[CrossRef](#)]
40. Grieger, J.C.; Snowdy, S.; Samulski, R.J. Separate Basic Region Motifs within the Adeno-Associated Virus Capsid Proteins Are Essential for Infectivity and Assembly. *J. Virol.* **2006**, *80*, 5199–5210. [[CrossRef](#)] [[PubMed](#)]
41. Sonntag, F.; Bleker, S.; Leuchs, B.; Fischer, R.; Kleinschmidt, J.A. Adeno-Associated Virus Type 2 Capsids with Externalized VP1/VP2 Trafficking Domains Are Generated Prior to Passage through the Cytoplasm and Are Maintained until Uncoating Occurs in the Nucleus. *J. Virol.* **2006**, *80*, 11040–11054. [[CrossRef](#)]
42. Mäntylä, E.; Aho, V.; Kann, M.; Vihinen-Ranta, M. Cytoplasmic Parvovirus Capsids Recruit Importin Beta for Nuclear Delivery. *J. Virol.* **2019**, *94*. [[CrossRef](#)]
43. Fay, N.; Panté, N. Old Foes, New Understandings: Nuclear Entry of Small Non-Enveloped DNA Viruses. *Curr. Opin. Virol.* **2015**, *12*, 59–65. [[CrossRef](#)] [[PubMed](#)]
44. Tattersall, P.; Ward, D.C. Rolling Hairpin Model for Replication of Parvovirus and Linear Chromosomal DNA. *Nature* **1976**, *263*, 106–109. [[CrossRef](#)] [[PubMed](#)]
45. Adeyemi, R.O.; Landry, S.; Davis, M.E.; Weitzman, M.D.; Pintel, D.J. Parvovirus Minute Virus of Mice Induces a DNA Damage Response That Facilitates Viral Replication. *PLoS Pathog.* **2010**, *6*, 1001141. [[CrossRef](#)] [[PubMed](#)]
46. Bashir, T.; Rommelaere, J.; Cziepluch, C. In Vivo Accumulation of Cyclin A and Cellular Replication Factors in Autonomous Parvovirus Minute Virus of Mice-Associated Replication Bodies. *J. Virol.* **2001**, *75*, 4394–4398. [[CrossRef](#)] [[PubMed](#)]
47. Ihalainen, T.O.; Niskanen, E.A.; Jylhävä, J.; Paloheimo, O.; Dross, N.; Smolander, H.; Langowski, J.; Timonen, J.; Vihinen-Ranta, M. Parvovirus Induced Alterations in Nuclear Architecture and Dynamics. *PLoS ONE* **2009**, *4*. [[CrossRef](#)]
48. Adeyemi, R.O.; Pintel, D.J. Replication of Minute Virus of Mice in Murine Cells Is Facilitated by Virally Induced Depletion of P21. *J. Virol.* **2012**, *86*, 8328–8332. [[CrossRef](#)]
49. Adeyemi, R.O.; Pintel, D.J. Parvovirus-Induced Depletion of Cyclin B1 Prevents Mitotic Entry of Infected Cells. *PLoS Pathog.* **2014**, *10*, 1003891. [[CrossRef](#)]
50. Lou, S.; Luo, Y.; Cheng, F.; Huang, Q.; Shen, W.; Kleiboeker, S.; Tisdale, J.F.; Liu, Z.; Qiu, J. Human Parvovirus B19 DNA Replication Induces a DNA Damage Response That Is Dispensable for Cell Cycle Arrest at Phase G2/M. *J. Virol.* **2012**, *86*, 10748–10758. [[CrossRef](#)]
51. Majumder, K.; Etingov, I.; Pintel, D.J. Protoparvovirus Interactions with the Cellular DNA Damage Response. *Viruses* **2017**, *9*, 323. [[CrossRef](#)]
52. Majumder, K.; Wang, J.; Boftsi, M.; Fuller, M.S.; Rede, J.E.; Joshi, T.; Pintel, D.J. Parvovirus Minute Virus of Mice Interacts with Sites of Cellular DNA Damage to Establish and Amplify Its Lytic Infection. *eLife* **2018**, *7*. [[CrossRef](#)]
53. Cotmore, S.F.; Tattersall, P. Parvoviruses: Small Does Not Mean Simple. *Annu. Rev. Virol.* **2014**, *1*, 517–537. [[CrossRef](#)]
54. Op De Beeck, A.; Caillet-Fauquet, P. The NS1 Protein of the Autonomous Parvovirus Minute Virus of Mice Blocks Cellular DNA Replication: A Consequence of Lesions to the Chromatin? *J. Virol.* **1997**, *71*, 5323–5329. [[CrossRef](#)]
55. Moffatt, S.; Yaegashi, N.; Tada, K.; Tanaka, N.; Sugamura, K. Human Parvovirus B19 Nonstructural (NS1) Protein Induces Apoptosis in Erythroid Lineage Cells. *J. Virol.* **1998**, *72*, 3018–3028. [[CrossRef](#)] [[PubMed](#)]
56. Chen, A.Y.; Qiu, J. Parvovirus Infection-Induced Cell Death and Cell Cycle Arrest. *Future Virol.* **2010**, *5*, 731–743. [[CrossRef](#)]
57. Cotmore, S.F.; Tattersall, P. Parvovirus Diversity and DNA Damage Responses. *Cold Spring Harb. Perspect. Biol.* **2013**, *5*. [[CrossRef](#)] [[PubMed](#)]
58. Lombardo, E.; Ramírez, J.C.; Agbandje-McKenna, M.; Almendral, J.M. A Beta-Stranded Motif Drives Capsid Protein Oligomers of the Parvovirus Minute Virus of Mice into the Nucleus for Viral Assembly. *J. Virol.* **2000**, *74*, 3804–3814. [[CrossRef](#)]
59. Riolobos, L.; Reguera, J.; Mateu, M.G.; Almendral, J.M. Nuclear Transport of Trimeric Assembly Intermediates Exerts a Morphogenetic Control on the Icosahedral Parvovirus Capsid. *J. Mol. Biol.* **2006**, *357*, 1026–1038. [[CrossRef](#)]
60. Gil-Ranedo, J.; Hernando, E.; Riolobos, L.; Domínguez, C.; Kann, M.; Almendral, J.M. The Mammalian Cell Cycle Regulates Parvovirus Nuclear Capsid Assembly. *PLoS Pathog.* **2015**, *11*, e1004920. [[CrossRef](#)] [[PubMed](#)]
61. Russell, D.W.; Miller, A.D.; Alexander, I.E. Adeno-Associated Virus Vectors Preferentially Transduce Cells in S Phase. *Proc. Natl. Acad. Sci. USA* **1994**, *91*, 8915–8919. [[CrossRef](#)] [[PubMed](#)]
62. Bartlett, J.S.; Wilcher, R.; Samulski, R.J. Infectious Entry Pathway of Adeno-Associated Virus and Adeno-Associated Virus Vectors. *J. Virol.* **2000**, *74*, 2777–2785. [[CrossRef](#)] [[PubMed](#)]
63. Vihinen-Ranta, M.; Yuan, W.; Parrish, C.R. Cytoplasmic Trafficking of the Canine Parvovirus Capsid and Its Role in Infection and Nuclear Transport. *J. Virol.* **2000**, *74*, 4853–4859. [[CrossRef](#)] [[PubMed](#)]

64. Seisenberger, G.; Ried, M.U.; Endreß, T.; Büning, H.; Hallek, M.; Bräuchle, C. Real-Time Single-Molecule Imaging of the Infection Pathway of Adeno-Associated Virus. *Science* **2001**, *294*, 1929–1932. [[CrossRef](#)]
65. Lee, D.W.; Allison, A.B.; Bacon, K.B.; Parrish, C.R.; Daniel, S. Single-Particle Tracking Shows That a Point Mutation in the Carnivore Parvovirus Capsid Switches Binding between Host-Specific Transferrin Receptors. *J. Virol.* **2016**, *90*, 4849–4853. [[CrossRef](#)]
66. Cureton, D.K.; Harbison, C.E.; Cocucci, E.; Parrish, C.R.; Kirchhausen, T. Limited Transferrin Receptor Clustering Allows Rapid Diffusion of Canine Parvovirus into Clathrin Endocytic Structures. *J. Virol.* **2012**, *86*, 5330–5340. [[CrossRef](#)]
67. Xiao, P.-J.; Samulski, R.J. Cytoplasmic Trafficking, Endosomal Escape, and Perinuclear Accumulation of Adeno-Associated Virus Type 2 Particles Are Facilitated by Microtubule Network. *J. Virol.* **2012**, *86*, 10462–10473. [[CrossRef](#)]
68. Saxton, M.J. A Biological Interpretation of Transient Anomalous Subdiffusion. I. Qualitative Model. *Biophys. J.* **2007**, *92*, 1178–1191. [[CrossRef](#)]
69. Warrington, K.H.; Gorbatyuk, O.S.; Harrison, J.K.; Opie, S.R.; Zolotukhin, S.; Muzyczka, N. Adeno-Associated Virus Type 2 VP2 Capsid Protein Is Nonessential and Can Tolerate Large Peptide Insertions at Its N Terminus. *J. Virol.* **2004**, *78*, 6595–6609. [[CrossRef](#)]
70. Lux, K.; Goerlitz, N.; Schlemminger, S.; Perabo, L.; Goldnau, D.; Endell, J.; Leike, K.; Kofler, D.M.; Finke, S.; Hallek, M.; et al. Green Fluorescent Protein-Tagged Adeno-Associated Virus Particles Allow the Study of Cytosolic and Nuclear Trafficking. *J. Virol.* **2005**, *79*, 11776–11787. [[CrossRef](#)]
71. Chandran, J.S.; Sharp, P.S.; Karyka, E.; Aves-Cruzeiro, J.M.D.C.; Coldicott, I.; Castelli, L.; Hautbergue, G.; Collins, M.O.; Azzouz, M. Site Specific Modification of Adeno-Associated Virus Enables Both Fluorescent Imaging of Viral Particles and Characterization of the Capsid Interactome. *Sci. Rep.* **2017**, *7*, 1–17. [[CrossRef](#)]
72. Michelfelder, S.; Varadi, K.; Raupp, C.; Hunger, A.; Körbelin, J.; Pahrman, C.; Schrepfer, S.; Müller, O.J.; Kleinschmidt, J.A.; Trepel, M. Peptide Ligands Incorporated into the Threefold Spike Capsid Domain to Re-Direct Gene Transduction of AAV8 and AAV9 in Vivo. *PLoS ONE* **2011**, *6*, e23101. [[CrossRef](#)]
73. Digman, M.A.; Gratton, E. Lessons in Fluctuation Correlation Spectroscopy. *Annu. Rev. Phys. Chem.* **2011**, *62*, 645–668. [[CrossRef](#)]
74. Hinde, E.; Cardarelli, F.; Digman, M.A.; Gratton, E. In Vivo Pair Correlation Analysis of EGFP Intranuclear Diffusion Reveals DNA-Dependent Molecular Flow. *Proc. Natl. Acad. Sci. USA* **2010**, *107*, 16560–16565. [[CrossRef](#)] [[PubMed](#)]
75. Digman, M.A.; Gratton, E. Imaging Barriers to Diffusion by Pair Correlation Functions. *Biophys. J.* **2009**, *97*, 665–673. [[CrossRef](#)] [[PubMed](#)]
76. Liang, L.; Wang, X.; Xing, D.; Chen, T.; Chen, W.R. Noninvasive Determination of Cell Nucleoplasmic Viscosity by Fluorescence Correlation Spectroscopy. *J. Biomed. Opt.* **2009**, *14*, 024013. [[CrossRef](#)]
77. Seksek, O.; Biwersi, J.; Verkman, A.S. Translational Diffusion of Macromolecule-Sized Solute in Cytoplasm and Nucleus. *J. Cell Biol.* **1997**, *138*, 131–142. [[CrossRef](#)] [[PubMed](#)]
78. Ros, C.; Baltzer, C.; Mani, B.; Kempf, C. Parvovirus Uncoating in Vitro Reveals a Mechanism of DNA Release without Capsid Disassembly and Striking Differences in Encapsidated DNA Stability. *Virology* **2006**, *345*, 137–147. [[CrossRef](#)] [[PubMed](#)]
79. Mani, B.; Baltzer, C.; Valle, N.; Almendral, J.M.; Kempf, C.; Ros, C. Low pH-Dependent Endosomal Processing of the Incoming Parvovirus Minute Virus of Mice Virion Leads to Externalization of the VP1 N-Terminal Sequence (N-VP1), N-VP2 Cleavage, and Uncoating of the Full-Length Genome. *J. Virol.* **2006**, *80*, 1015–1024. [[CrossRef](#)]
80. Suikkanen, S.; Antila, M.; Jaatinen, A.; Vihinen-Ranta, M.; Vuento, M. Release of Canine Parvovirus from Endocytic Vesicles. *Virology* **2003**, *316*, 267–280. [[CrossRef](#)]
81. Caliaro, O.; Marti, A.; Ruprecht, N.; Leisi, R.; Subramanian, S.; Hafenstein, S.; Ros, C. Parvovirus B19 Uncoating Occurs in the Cytoplasm without Capsid Disassembly and It Is Facilitated by Depletion of Capsid-Associated Divalent Cations. *Viruses* **2019**, *11*, 430. [[CrossRef](#)]
82. Cotmore, S.F.; D’Abramo, A.M.; Ticknor, C.M.; Tattersall, P. Controlled Conformational Transitions in the MVM Virion Expose the VP1 N-Terminus and Viral Genome without Particle Disassembly. *Virology* **1999**, *254*, 169–181. [[CrossRef](#)] [[PubMed](#)]
83. Cotmore, S.F.; Hafenstein, S.; Tattersall, P. Depletion of Virion-Associated Divalent Cations Induces Parvovirus Minute Virus of Mice to Eject Its Genome in a 3′-to-5′ Direction from an Otherwise Intact Viral Particle. *J. Virol.* **2010**, *84*, 1945–1956. [[CrossRef](#)]
84. Cotmore, S.F.; Tattersall, P. Mutations at the Base of the Icosahedral Five-Fold Cylinders of Minute Virus of Mice Induce 3′-to-5′ Genome Uncoating and Critically Impair Entry Functions. *J. Virol.* **2012**, *86*, 69–80. [[CrossRef](#)] [[PubMed](#)]
85. Ros, C.; Kempf, C. The Ubiquitin-Proteasome Machinery Is Essential for Nuclear Translocation of Incoming Minute Virus of Mice. *Virology* **2004**, *324*, 350–360. [[CrossRef](#)]
86. Bernaud, J.; Rossi, A.; Fis, A.; Gardette, L.; Aillot, L.; Büning, H.; Castelnovo, M.; Salvetti, A.; Faivre-Moskalenko, C. Characterization of AAV Vector Particle Stability at the Single-Capsid Level. *J. Biol. Phys.* **2018**, *44*, 181–194. [[CrossRef](#)]
87. Cziepluch, C.; Lampel, S.; Grewenig, A.; Grund, C.; Lichter, P.; Rommelaere, J. H-1 Parvovirus-Associated Replication Bodies: A Distinct Virus-Induced Nuclear Structure. *J. Virol.* **2000**, *74*, 4807–4815. [[CrossRef](#)]
88. Mäntylä, E.; Salokas, K.; Oittinen, M.; Aho, V.; Mäntysaari, P.; Palmujoki, L.; Kalliollinna, O.; Ihalainen, T.O.; Niskanen, E.A.; Timonen, J.; et al. Promoter-Targeted Histone Acetylation of Chromatinized Parvoviral Genome Is Essential for the Progress of Infection. *J. Virol.* **2016**, *90*, 4059–4066. [[CrossRef](#)] [[PubMed](#)]

89. Ihalainen, T.O.; Willman, S.F.; Niskanen, E.A.; Paloheimo, O.; Smolander, H.; Laurila, J.P.; Kaikkonen, M.U.; Vihinen-Ranta, M. Distribution and Dynamics of Transcription-Associated Proteins during Parvovirus Infection. *J. Virol.* **2012**, *86*, 13779–13784. [[CrossRef](#)] [[PubMed](#)]
90. Ihalainen, T.O.; Niskanen, E.A.; Jylhävä, J.; Turpeinen, T.; Rinne, J.; Timonen, J.; Vihinen-Ranta, M. Dynamics and Interactions of Parvoviral NS1 Protein in the Nucleus. *Cell. Microbiol.* **2007**, *9*, 1946–1959. [[CrossRef](#)] [[PubMed](#)]
91. Riolobos, L.; Valle, N.; Hernando, E.; Maroto, B.; Kann, M.; Almendral, J.M. Viral Oncolysis That Targets Raf-1 Signaling Control of Nuclear Transport. *J. Virol.* **2010**, *84*, 2090–2099. [[CrossRef](#)]
92. Wistuba, A.; Kern, A.; Weger, S.; Grimm, D.; Kleinschmidt, J.A. Subcellular Compartmentalization of Adeno-Associated Virus Type 2 Assembly. *J. Virol.* **1997**, *71*, 1341–1352. [[CrossRef](#)] [[PubMed](#)]
93. Naumer, M.; Sonntag, F.; Schmidt, K.; Nieto, K.; Panke, C.; Davey, N.E.; Popa-Wagner, R.; Kleinschmidt, J.A. Properties of the Adeno-Associated Virus Assembly-Activating Protein. *J. Virol.* **2012**, *86*, 13038–13048. [[CrossRef](#)] [[PubMed](#)]
94. Plevka, P.; Hafenstein, S.; Li, L.; D’Abramo, A.; Cotmore, S.F.; Rossmann, M.G.; Tattersall, P. Structure of a Packaging-Defective Mutant of Minute Virus of Mice Indicates That the Genome Is Packaged via a Pore at a 5-Fold Axis. *J. Virol.* **2011**, *85*, 4822–4827. [[CrossRef](#)] [[PubMed](#)]
95. Subramanian, S.; Organtini, L.J.; Grossman, A.; Domeier, P.P.; Cifuentes, J.O.; Makhov, A.M.; Conway, J.F.; D’Abramo, A.; Cotmore, S.F.; Tattersall, P.; et al. Cryo-EM Maps Reveal Five-Fold Channel Structures and Their Modification by Gatekeeper Mutations in the Parvovirus Minute Virus of Mice (MVM) Capsid. *Virology* **2017**, *510*, 216–223. [[CrossRef](#)]
96. Maroto, B.; Valle, N.; Saffrich, R.; Almendral, J.M. Nuclear Export of the Nonenveloped Parvovirus Virion Is Directed by an Unordered Protein Signal Exposed on the Capsid Surface. *J. Virol.* **2004**, *78*, 10685–10694. [[CrossRef](#)] [[PubMed](#)]
97. Köhler, A.; Hurt, E. Exporting RNA from the Nucleus to the Cytoplasm. *Nat. Rev. Mol. Cell Biol.* **2007**, *8*, 761–773. [[CrossRef](#)] [[PubMed](#)]
98. Panté, N.; Kann, M. Nuclear Pore Complex Is Able to Transport Macromolecules with Diameters of 39 Nm. *Mol. Biol. Cell* **2002**, *13*, 425–434. [[CrossRef](#)]
99. Nicolson, S.C.; Samulski, R.J. Recombinant Adeno-Associated Virus Utilizes Host Cell Nuclear Import Machinery to Enter the Nucleus. *J. Virol.* **2014**, *88*, 4132–4144. [[CrossRef](#)]
100. Söderberg, O.; Leuchowius, K.J.; Gullberg, M.; Jarvius, M.; Weibrecht, I.; Larsson, L.G.; Landegren, U. Characterizing Proteins and Their Interactions in Cells and Tissues Using the in Situ Proximity Ligation Assay. *Methods* **2008**, *45*, 227–232. [[CrossRef](#)]
101. Gerold, G.; Bruening, J.; Pietschmann, T. Decoding Protein Networks during Virus Entry by Quantitative Proteomics. *Virus Res.* **2016**, *218*, 25–39. [[CrossRef](#)] [[PubMed](#)]
102. Richards, A.L.; Eckhardt, M.; Krogan, N.J. Mass Spectrometry-based Protein–Protein Interaction Networks for the Study of Human Diseases. *Mol. Syst. Biol.* **2021**, *17*, e8792. [[CrossRef](#)] [[PubMed](#)]
103. Pankow, S.; Bamberger, C.; Calzolari, D.; Bamberger, A.; Yates, J.R. Deep Interactome Profiling of Membrane Proteins by Co-Interacting Protein Identification Technology. *Nat. Protoc.* **2016**, *11*, 2515–2528. [[CrossRef](#)] [[PubMed](#)]
104. Kovács, I.A.; Luck, K.; Spirohn, K.; Wang, Y.; Pollis, C.; Schlabach, S.; Bian, W.; Kim, D.K.; Kishore, N.; Hao, T.; et al. Network-Based Prediction of Protein Interactions. *Nat. Commun.* **2019**, *10*, 1–8. [[CrossRef](#)]
105. Silverbush, D.; Sharan, R. A Systematic Approach to Orient the Human Protein–Protein Interaction Network. *Nat. Commun.* **2019**, *10*, 1–9. [[CrossRef](#)] [[PubMed](#)]
106. Liu, Q.; Zheng, J.; Sun, W.; Huo, Y.; Zhang, L.; Hao, P.; Wang, H.; Zhuang, M. A Proximity-Tagging System to Identify Membrane Protein–Protein Interactions. *Nat. Methods* **2018**, *15*, 715–722. [[CrossRef](#)] [[PubMed](#)]
107. Roux, K.J.; Kim, D.I.; Raida, M.; Burke, B. A Promiscuous Biotin Ligase Fusion Protein Identifies Proximal and Interacting Proteins in Mammalian Cells. *J. Cell Biol.* **2012**, *196*, 801–810. [[CrossRef](#)]
108. Sears, R.M.; May, D.G.; Roux, K.J. BioID as a tool for protein-proximity labeling in living cells. *Methods Mol. Biol.* **2019**. [[CrossRef](#)]
109. Liu, X.; Salokas, K.; Tamene, F.; Jiu, Y.; Weldatsadik, R.G.; Öhman, T.; Varjosalo, M. An AP-MS- and BioID-Compatible MAC-Tag Enables Comprehensive Mapping of Protein Interactions and Subcellular Localizations. *Nat. Commun.* **2018**, *9*, 1–16. [[CrossRef](#)]
110. Wang, X.; Xu, P.; Cheng, F.; Li, Y.; Wang, Z.; Hao, S.; Wang, J.; Ning, K.; Ganaie, S.S.; Engelhardt, J.F.; et al. Cellular Cleavage and Polyadenylation Specificity Factor 6 (CPSF6) Mediates Nuclear Import of Human Bocavirus 1 NP1 Protein and Modulates Viral Capsid Protein Expression. *J. Virol.* **2020**, *94*. [[CrossRef](#)]
111. Smith-Moore, S.; Neil, S.J.D.; Fraefel, C.; Michael Linden, R.; Bollen, M.; Rowe, H.M.; Henckaerts, E. Adeno-Associated Virus Rep Proteins Antagonize Phosphatase PP1 to Counteract KAP1 Repression of the Latent Viral Genome. *Proc. Natl. Acad. Sci. USA* **2018**, *115*, E3529–E3538. [[CrossRef](#)]
112. Mattola, S.; Salokas, K.; Aho, V.; Hakanen, S.; Salminen, S.; Mäntylä, E.; Niskanen, E.A.; Svirskaitė, J.; Ihalainen, T.O.; Parrish, C.R.; et al. Parvovirus Nonstructural Protein 2 Interacts with Proteins of Cellular Machinery Regulating Chromatin Functions (Manuscript).
113. Lilley, C.E.; Schwartz, R.A.; Weitzman, M.D. Using or Abusing: Viruses and the Cellular DNA Damage Response. *Trends Microbiol.* **2007**, *15*, 119–126. [[CrossRef](#)]
114. Trigg, B.J.; Ferguson, B.J. Functions of DNA Damage Machinery in the Innate Immune Response to DNA virus Infection. *Curr. Opin. Virol.* **2015**, *15*, 56–62. [[CrossRef](#)]
115. Kastan, M.B.; Bartek, J. Cell-Cycle Checkpoints and Cancer. *Nature* **2004**, *432*, 316–323. [[CrossRef](#)]

116. Shiotani, B.; Zou, L. Single-Stranded DNA Orchestrates an ATM-to-ATR Switch at DNA Breaks. *Mol. Cell* **2009**, *33*, 547–558. [[CrossRef](#)] [[PubMed](#)]
117. Deng, X.; Yan, Z.; Cheng, F.; Engelhardt, J.F.; Qiu, J. Replication of an Autonomous Human Parvovirus in Non-Dividing Human Airway Epithelium Is Facilitated through the DNA Damage and Repair Pathways. *PLoS Pathog.* **2016**, *12*. [[CrossRef](#)]
118. Luo, Y.; Lou, S.; Deng, X.; Liu, Z.; Li, Y.; Kleiboeker, S.; Qiu, J. Parvovirus B19 Infection of Human Primary Erythroid Progenitor Cells Triggers ATR-Chk1 Signaling, Which Promotes B19 Virus Replication. *J. Virol.* **2011**, *85*, 8046–8055. [[CrossRef](#)]
119. Schwartz, R.A.; Carson, C.T.; Schubert, C.; Weitzman, M.D. Adeno-Associated Virus Replication Induces a DNA Damage Response Coordinated by DNA-Dependent Protein Kinase. *J. Virol.* **2009**, *83*, 6269–6278. [[CrossRef](#)] [[PubMed](#)]
120. Vassin, V.M.; Anantha, R.W.; Sokolova, E.; Kanner, S.; Borowiec, J.A. Human RPA Phosphorylation by ATR Stimulates DNA Synthesis and Prevents SsDNA Accumulation during DNA-Replication Stress. *J. Cell Sci.* **2009**, *122*, 4070–4080. [[CrossRef](#)] [[PubMed](#)]
121. Majumder, K.; Boftsi, M.; Whittle, F.B.; Wang, J.; Fuller, M.S.; Joshi, T.; Pintel, D.J. The NS1 Protein of the Parvovirus MVM Aids in the Localization of the Viral Genome to Cellular Sites of DNA Damage. *PLoS Pathog.* **2020**, *16*, e1009002. [[CrossRef](#)] [[PubMed](#)]
122. Dixon, J.R.; Gorkin, D.U.; Ren, B. Chromatin Domains: The Unit of Chromosome Organization. *Mol. Cell* **2016**, *62*, 668–680. [[CrossRef](#)] [[PubMed](#)]
123. Ostling, O.; Johanson, K.J. Microelectrophoretic Study of Radiation-Induced DNA Damages in Individual Mammalian Cells. *Biochem. Biophys. Res. Commun.* **1984**, *123*, 291–298. [[CrossRef](#)]
124. Olive, P.L.; Banáth, J.P. The Comet Assay: A Method to Measure DNA Damage in Individual Cells. *Nat. Protoc.* **2006**, *1*, 23–29. [[CrossRef](#)]
125. Collins, A.R. The Comet Assay: A Heavenly Method! *Mutagenesis* **2015**, *30*, 1–4. [[CrossRef](#)]
126. Alekseev, O.; Donegan, W.E.; Donovan, K.R.; Limonnik, V.; Azizkhan-Clifford, J. HSV-1 Hijacks the Host Dna Damage Response in Corneal Epithelial Cells through ICP4-Mediated Activation of ATM. *Invest. Ophthalmol. Vis. Sci.* **2020**, *61*, 39. [[CrossRef](#)] [[PubMed](#)]
127. Luo, Y.; Kleiboeker, S.; Deng, X.; Qiu, J. Human Parvovirus B19 Infection Causes Cell Cycle Arrest of Human Erythroid Progenitors at Late S Phase That Favors Viral DNA Replication. *J. Virol.* **2013**, *87*, 12766–12775. [[CrossRef](#)]
128. Goodwin, S.; McPherson, J.D.; McCombie, W.R. Coming of Age: Ten Years of next-Generation Sequencing Technologies. *Nat. Rev. Genet.* **2016**, *17*, 333–351. [[CrossRef](#)]
129. Metzker, M.L. Sequencing Technologies the next Generation. *Nat. Rev. Genet.* **2010**, *11*, 31–46. [[CrossRef](#)] [[PubMed](#)]
130. Marx, V. Method of the Year: Spatially Resolved Transcriptomics. *Nat. Methods* **2021**, *18*, 9–14. [[CrossRef](#)] [[PubMed](#)]
131. Stickels, R.R.; Murray, E.; Kumar, P.; Li, J.; Marshall, J.L.; Di Bella, D.J.; Arlotta, P.; Macosko, E.Z.; Chen, F. Highly Sensitive Spatial Transcriptomics at Near-Cellular Resolution with Slide-SeqV2. *Nat. Biotechnol.* **2021**, *39*, 313–319. [[CrossRef](#)] [[PubMed](#)]
132. Larsson, L.; Frisé, J.; Lundeberg, J. Spatially Resolved Transcriptomics Adds a New Dimension to Genomics. *Nat. Methods* **2021**, *18*, 15–18. [[CrossRef](#)]
133. Zhuang, X. Spatially Resolved Single-Cell Genomics and Transcriptomics by Imaging. *Nat. Methods* **2021**, *18*, 18–22. [[CrossRef](#)]
134. Wang, Z.; Gerstein, M.; Snyder, M. RNA-Seq: A Revolutionary Tool for Transcriptomics. *Nat. Rev. Genet.* **2009**, *10*, 57–63. [[CrossRef](#)] [[PubMed](#)]
135. Buenrostro, J.D.; Giresi, P.G.; Zaba, L.C.; Chang, H.Y.; Greenleaf, W.J. Transposition of Native Chromatin for Fast and Sensitive Epigenomic Profiling of Open Chromatin, DNA-Binding Proteins and Nucleosome Position. *Nat. Methods* **2013**, *10*, 1213–1218. [[CrossRef](#)]
136. Aughey, G.N.; Cheetham, S.W.; Southall, T.D. DamID as a Versatile Tool for Understanding Gene Regulation. *Dev. Camb.* **2019**, *146*. [[CrossRef](#)] [[PubMed](#)]
137. Kaya-Okur, H.S.; Wu, S.J.; Codomo, C.A.; Pledger, E.S.; Bryson, T.D.; Henikoff, J.G.; Ahmad, K.; Henikoff, S. CUT&Tag for Efficient Epigenomic Profiling of Small Samples and Single Cells. *Nat. Commun.* **2019**, *10*, 1–10. [[CrossRef](#)]
138. Furey, T.S. ChIP-Seq and beyond: New and Improved Methodologies to Detect and Characterize Protein-DNA Interactions. *Nat. Rev. Genet.* **2012**, *13*, 840–852. [[CrossRef](#)] [[PubMed](#)]
139. De Wit, E.; de Laat, W. A Decade of 3C Technologies: Insights into Nuclear Organization. *Genes Dev.* **2012**, *26*, 11–24. [[CrossRef](#)]
140. Kong, X.; Wei, G.; Chen, N.; Zhao, S.; Shen, Y.; Zhang, J.; Li, Y.; Zeng, X.; Wu, X. Dynamic Chromatin Accessibility Profiling Reveals Changes in Host Genome Organization in Response to Baculovirus Infection. *PLoS Pathog.* **2020**, *16*, e1008633. [[CrossRef](#)]
141. Lamontagne, R.J.; Soldan, S.S.; Su, C.; Wiedmer, A.; Won, K.J.; Lu, F.; Goldman, A.R.; Wickramasinghe, J.; Tang, H.Y.; Speicher, D.W.; et al. A Multi-Omics Approach to Epstein-Barr Virus Immortalization of B-Cells Reveals EBNA1 Chromatin Pioneering Activities Targeting Nucleotide Metabolism. *PLoS Pathog.* **2021**, *17*, e1009208. [[CrossRef](#)]
142. Van Steensel, B.; Henikoff, S. Identification of in Vivo DNA Targets of Chromatin Proteins Using Tethered Dam Methyltransferase. *Nat. Biotechnol.* **2000**, *18*, 424–428. [[CrossRef](#)]
143. Kind, J.; Pagie, L.; De Vries, S.S.; Nahidiazar, L.; Dey, S.S.; Bienko, M.; Zhan, Y.; Lajoie, B.; De Graaf, C.A.; Amendola, M.; et al. Genome-Wide Maps of Nuclear Lamina Interactions in Single Human Cells. *Cell* **2015**, *163*, 134–147. [[CrossRef](#)]
144. Chen, X.; Shen, Y.; Draper, W.; Buenrostro, J.D.; Litzenger, U.; Cho, S.W.; Satpathy, A.T.; Carter, A.C.; Ghosh, R.P.; East-Seletsky, A.; et al. ATAC-See Reveals the Accessible Genome by Transposase-Mediated Imaging and Sequencing. *Nat. Methods* **2016**, *13*, 1013–1020. [[CrossRef](#)] [[PubMed](#)]

-
145. Kind, J.; Pagie, L.; Ortabozkoyun, H.; Boyle, S.; De Vries, S.S.; Janssen, H.; Amendola, M.; Nolen, L.D.; Bickmore, W.A.; Van Steensel, B. Single-Cell Dynamics of Genome-Nuclear Lamina Interactions. *Cell* **2013**, *153*, 178–192. [[CrossRef](#)] [[PubMed](#)]
 146. Takei, Y.; Yun, J.; Zheng, S.; Ollikainen, N.; Pierson, N.; White, J.; Shah, S.; Thomassie, J.; Suo, S.; Eng, C.H.L.; et al. Integrated Spatial Genomics Reveals Global Architecture of Single Nuclei. *Nature* **2021**, *590*, 344–350. [[CrossRef](#)] [[PubMed](#)]